

# The Role of Feedback in Shaping the Structure of the Interstellar Medium

A.P. Walker<sup>1</sup>, B.K. Gibson<sup>1,2</sup>, K. Pilkington<sup>1,2</sup>, C.B. Brook<sup>3,1</sup>, P. Dutta<sup>4</sup>,  
S. Stanimirović<sup>5</sup>, G.S. Stinson<sup>6</sup>, and J. Bailin<sup>7</sup>

<sup>1</sup>*Jeremiah Horrocks Institute, University of Central Lancashire, Preston, PR1 2HE, UK*

<sup>2</sup>*Institute for Computational Astrophysics, Dept of Astronomy & Physics, Saint Mary's University, Halifax, NS, B3H 3C3, Canada*

<sup>3</sup>*Departamento de Física Teórica, Universidad Autónoma de Madrid, E-28049 Cantoblanco, Madrid, Spain*

<sup>4</sup>*National Centre for Radio Astrophysics, Post Bag 3, Ganeshkhind, Pune, 411 007, India*

<sup>5</sup>*Department of Astronomy, University of Wisconsin, 475 North Charter St., Madison, WI, 53706, USA*

<sup>6</sup>*Max-Planck-Institut für Astronomie, Königstuhl 17, 69117 Heidelberg, Germany*

<sup>7</sup>*Department of Physics & Astronomy, University of Alabama, Tuscaloosa, AL, 35487-0324, USA*

Accepted: 3 March 2014

## ABSTRACT

We present an analysis of the role of feedback in shaping the neutral hydrogen (HI) content of simulated disc galaxies. For our analysis, we have used two realisations of two separate Milky Way-like ( $\sim L_\star$ ) discs - one employing a conservative feedback scheme (MUGS), the other significantly more energetic (MaGICC). To quantify the impact of these schemes, we generate zeroth moment (surface density) maps of the inferred HI distribution; construct power spectra associated with the underlying structure of the simulated cold ISM, in addition to their radial surface density and velocity dispersion profiles. Our results are compared with a parallel, self-consistent, analysis of empirical data from THINGS (The HI Nearby Galaxy Survey). Single power-law fits ( $P \propto k^\gamma$ ) to the power spectra of the stronger-feedback (MaGICC) runs (over spatial scales corresponding to  $\sim 0.5$  kpc to  $\sim 20$  kpc) result in slopes consistent with those seen in the THINGS sample ( $\gamma \sim -2.5$ ). The weaker-feedback (MUGS) runs exhibit shallower power law slopes ( $\gamma \sim -1.2$ ). The power spectra of the MaGICC simulations are more consistent though with a two-component fit, with a flatter distribution of power on larger scales (i.e.,  $\gamma \sim -1.4$  for scales in excess of  $\sim 2$  kpc) and a steeper slope on scales below  $\sim 1$  kpc ( $\gamma \sim -5$ ), qualitatively consistent with empirical claims, as well as our earlier work on dwarf discs. The radial HI surface density profiles of the MaGICC discs show a clear exponential behaviour, while those of the MUGS suite are essentially flat; both behaviours are encountered in nature, although the THINGS sample is more consistent with our stronger (MaGICC) feedback runs.

**Key words:** ISM: structure – galaxies: evolution – galaxies: formation – galaxies: spiral – methods: N-body simulations

## 1 INTRODUCTION

The feedback of energy into the interstellar medium (ISM) is a fundamental factor in shaping the morphology, kinematics, and chemistry of galaxies, both in nature and in their simulated analogues (e.g. Thacker & Couchman 2000; Governato et al. 2010; Schaye et al. 2010; Hambleton et al. 2011; Brook et al. 2012; Scannapieco et al. 2012; Durier & Dalla Vecchia 2012; Hopkins et al. 2013, and references therein). Perhaps the single-most frustrating impediment to realising accurate realisations of simulated galaxies is the spatial ‘mismatch’ between the sub-pc scale on which star formation and feedback operates, and the

10s to 100s of pc scale accessible to modellers within a cosmological framework. Attempts to better constrain ‘sub-grid’ physics, on a macroscopic scale, have driven the field for more than a decade, and will likely continue to do so into the foreseeable future.

The efficiency and mechanism by which energy from massive stars (both explosive energy deposition from supernovae and pre-explosion radiation energy), cosmic rays, and magnetic fields couple to the ISM can be constrained indirectly via an array of empirical probes, including (but not limited to) stellar halo (Brook et al. 2004) and disc (Pilkington et al. 2012) metallicity distribution functions, statistical measures of galaxy light compact-

ness, asymmetry, and clumpiness (Hambleton et al. 2011), stellar disc age-velocity dispersion relations (House et al. 2011), rotation curves and density profiles of dwarf galaxies (Macciò et al. 2012), low- and high-redshift ‘global’ scaling relations (Brook et al. 2012), background QSO probes of the ionised circum-galactic medium (Stinson et al. 2012), and the spatial distribution of metals (e.g., abundance gradients and age-metallicity relations) throughout the stellar disc (Pilkington et al. 2012; Gibson et al. 2013).

In Pilkington et al. (2011), we explored an alternate means by which to assess the efficacy of energy feedback schemes within a cosmological context: specifically, the predicted distribution of structural ‘power’ encoded within the underlying cold gas of late-type *dwarf* galaxies. Empirically, star forming dwarfs present steep spatial power-law spectra ( $P \propto k^\gamma$ ) for their cold gas, with  $\gamma < -3$  on spatial scales  $\lesssim 1$  kpc (Stanimirovic et al. 1999; Combes et al. 2012), consistent with the slope expected when HI density fluctuations dominate the ISM structure, rather than turbulent velocity fluctuations (which dominate when isolating ‘thin’ velocity slices). Our simulated (dwarf) disc galaxies showed similarly steep ISM power-law spectra, albeit deviating somewhat from the simple, single, power-law seen by Stanimirovic et al.

In comparison, the cold gas of late-type *giant* galaxies appears to possess a more complex distribution of structural power. Dutta et al. (2013) demonstrate that while such massive discs also present comparably steep (if not steeper) power spectra on smaller scales ( $\gamma \sim -3$ , for  $\lesssim 1$  kpc), there is a strong tendency for the power to ‘flatten’ to significantly shallower slopes on larger scales ( $\gamma \sim -1.5$ , for  $\gtrsim 2$  kpc). Dutta et al. propose a scenario in which the steeper power law component is driven by three-dimensional turbulence in the ISM on scales smaller than a given galaxy’s scaleheight, while the flatter component is driven by two-dimensional turbulence in the plane of the galaxy’s disc.

In what follows, we build upon our earlier work on dwarf galaxies (Pilkington et al. 2011), utilising the Fourier domain approach outlined by Stanimirovic et al. (1999), but now applied to a set of four simulated massive ( $\sim L^*$ ) disc systems. The simulations have each been realised with both conventional (i.e., moderate) and enhanced (i.e., strong/efficient) energy feedback. The impact of the feedback prescriptions upon the distribution of power in the ISM of their respective neutral hydrogen (HI) discs will be used, in an attempt to constrain the uncertain implementation of sub-grid physics. HI moment maps will be generated for each simulation *and* (for consistency) massive disc from The HI Nearby Galaxy Survey (THINGS: Walter et al. 2008), to make a fairer comparison with the observational data.

In §2, the basic properties of the simulations are reviewed, including the means by which the HI moment maps, and associated Fourier domain power spectra, were analysed. The resulting radial surface density profiles, velocity dispersion profiles, and distributions of power in the corresponding cold interstellar media are described in §3. Our conclusions are presented in §4.

## 2 METHOD

### 2.1 Simulations

Two  $\sim L^*$  disc galaxies (**g1536**; **g15784**), drawn from the McMaster Unbiased Galaxy Survey (MUGS: Stinson et al. 2010) and realised with the Smoothed Particle Hydrodynamics (SPH) code GASOLINE (Wadsley et al. 2004), form the primary inputs to our analysis.<sup>1</sup> Two variants for each disc were generated, one employing ‘conventional’ feedback (MUGS) and one using our ‘enhanced’ feedback scheme (MaGICC: Making Galaxies In a Cosmological Context - Brook et al. 2012; Stinson et al. 2012).<sup>2</sup> These four massive disc simulations are referred to henceforth as **g1536-MUGS**, **g1536-MaGICC**, **g15784-MUGS**, and **g15784-MaGICC**, and form the primary suite to which the subsequent analysis has been employed. To provide a bridge to our earlier study of the ISM power spectra of dwarf galaxies (Pilkington et al. 2011), we have analysed an ancillary set of three simulated low-mass discs (§3.4). An in-depth discussion of the MUGS and MaGICC star formation and feedback prescriptions are provided in the aforementioned works, although a brief summary of the key characteristics follows now.

The MUGS runs assume a thermal feedback scheme in which  $4 \times 10^{50}$  erg per supernova (SN) is made available to heat the surrounding ISM (‘conventional’), while the MaGICC runs use  $10^{51}$  erg/SN (‘enhanced’). The MUGS simulations employ a Kroupa et al. (1993) initial mass function (IMF), while MaGICC use the more ‘top-heavy’ Chabrier (2003) form.<sup>3</sup> Radiation energy feedback from massive stars during their pre-SN phase (lasting  $\sim 4$  Myr) is included in the MaGICC runs, although it should be emphasised that the effective coupling efficiency is  $< 1\%$  (Brook et al. 2012; Stinson et al. 2013). For both MUGS and MaGICC, cooling is disabled for gas particles situated within a blast region of size  $\sim 100$  pc, for a time period of  $\sim 10$  Myr. Star formation is restricted to regions which are both sufficiently cool and dense (MUGS:  $> 1 \text{ cm}^{-3}$ ; MaGICC:  $> 9 \text{ cm}^{-3}$ ). Metal diffusion (Shen et al. 2010) is included in all runs.

Supplementing the above four massive disc simulations, we have included three lower mass dwarf discs: (a) SG2 and SG3 (Brook et al. 2012) were realised with the same star formation and feedback schemes as the MaGICC versions of **g1536** and **g15784**, respectively; the only difference lies in their initial conditions, where the former have been ‘scaled-down’ by an order of magnitude in mass; (b) DG1 (Governato et al. 2010), the low mass dwarf that formed the basis of our earlier work (Pilkington et al. 2011).

<sup>1</sup> The role of feedback in shaping the abundance gradients, metallicity distribution functions, and age-metallicity relations of these same four realisations has been presented recently by Gibson et al. (2013).

<sup>2</sup> To link the simulation nomenclature with their earlier appearances in the literature, the MUGS variants of **g1536** and **g15784** are as first presented by Stinson et al. (2010), and analysed subsequently by Pilkington et al. (2012) and Calura et al. (2012), while the MaGICC variant of **g1536** corresponds to the ‘Fiducial’ run in Stinson et al. (2013) (itself, essentially the same as **SG5LR**, as first described by Brook et al. 2012).

<sup>3</sup> The MUGS runs assumed that the global metallicity  $Z \equiv \text{O} + \text{Fe}$ , while those of MaGICC assume  $Z \equiv \text{O} + \text{Fe} + \text{C} + \text{N} + \text{Ne} + \text{Mg} + \text{Si}$ .

## 2.2 Analysis

The analysis which follows is based upon a comparison of the HI gas properties of the MUGS+MaGICC simulations with their empirical ‘analogues’, drawn from The HI Nearby Galaxy Survey (THINGS: Walter et al. 2008). We ‘view’ the simulations face-on and restrict the comparison to massive discs from THINGS which are also close to face-on. In practice, this has meant limiting the analysis to the same subsample as that used by Dutta et al. (2013). In contrast, our earlier work (Pilkington et al. 2011) focussed on low-mass dwarf galaxies, rather than massive discs; in that study, we found that the index of the simulated ISM power spectrum ( $\gamma$ , where  $P \propto k^\gamma$ ) was consistent, to first order, with that observed in dwarfs (on spatial scales  $\lesssim 1$  kpc) such as the Small Magellanic Cloud (i.e.,  $\gamma \sim -3.2$ ). Besides determining the slope of the ISM power spectra for our new suite of massive disc galaxy simulations, we will present the radial HI surface density and velocity dispersion profiles, and contrast them with empirical data from the literature, in a further attempt to shed light on the role of feedback in shaping their characteristics.

In what follows, we make use of zeroth- (surface density) and second- (velocity dispersion) moment maps of each simulation’s HI distribution (viewed, face-on), realised with the image processing package *TIPSY*.<sup>4</sup> The redshift  $z=0$  snapshots for each galaxy are first centred and aligned such that the angular momentum vector of the disc is aligned with the  $z$ -axis, and the neutral hydrogen fraction of each SPH particle inferred under the assumption of combined photo- and collisional-ionisation equilibrium. From the zeroth- (second-) moment maps, radial HI surface density (velocity dispersion) profiles were generated for each simulation and (near) face-on, late-type, disc from THINGS. Individual results for each will be presented in §3. It is worth noting that out of the THINGS galaxies presented in Figure 7, NGCs 3031, 5236, 5457 and 6946 are more extended than the VLA primary beam, resulting potentially in missing larger-scale information (Walter et al. 2008).

After Stanimirovic et al. (1999) and Pilkington et al. (2011), the Fourier Transform of each of the aforementioned zeroth-moment HI maps (both simulations and empirical THINGS data) was taken, with circular annuli in Fourier space then employed to derive the average power in the structure of the ISM on different spatial scales.

## 3 RESULTS

### 3.1 Moment Maps

The zeroth-moment HI maps for our four simulated  $\sim L^*$  late-type discs are shown in Fig 1, with the two MaGICC (MUGS) variants shown in the upper (lower) panels. Each panel spans  $100 \times 100$  kpc. The ‘dynamic range’ in HI column density in each panel is  $\sim 10^{19} \text{ cm}^{-2}$  to  $\sim 10^{21} \text{ cm}^{-2}$  - i.e., (roughly) the current observational lower and upper limits for HI (21cm) detection (Bigiel et al. 2008).

Even a cursory inspection of Fig 1 suggests that the

enhanced feedback employed within MaGICC results in significantly more extended HI discs, relative to the conventional feedback treatment within MUGS. Similarly, at these column densities, the eye is drawn to the enhanced structure on larger scales seen in the MaGICC runs (relative to the more locally ‘confined’ structure seen in MUGS). Both points will be returned to below in a more quantitative sense.

### 3.2 Radial Surface Density Profiles

From the face-on moment zero maps of Fig 1, radial HI surface density profiles were generated. These are reflected in Fig 2 with the MUGS and MaGICC variants for g1536 (g15784) shown in the left (right) panel. As for Fig 1, the dynamic range has been limited to  $\gtrsim 10^{19} \text{ cm}^{-2}$  ( $\gtrsim 10^5 M_\odot/\text{kpc}^2$ ), to reflect the (typical) limiting 21cm detection limit in surveys such as THINGS; conversely, the horizontal line in each panel corresponds to the empirical HI upper limit (also from THINGS) of  $\sim 10^{6.9} M_\odot \text{ kpc}^{-2}$ .

The MaGICC discs (plus symbols in both panels) possess exponential surface density profiles (in HI) with  $\sim 6\text{--}8$  kpc scalelengths. Conversely, the MUGS realisations are clearly more ‘compact’, with essentially ‘flat’ radial HI surface density profiles (each with  $\sim 10^{20} \text{ cm}^{-2}$ , independent of galactocentric radius), with an extremely ‘sharp’ HI edge at  $\sim 12\text{--}15$  kpc. At a limiting HI (21cm) column density of  $\sim 10^{19} \text{ cm}^{-2}$ , the MaGICC discs are  $\sim 2\text{--}3\times$  more extended than their MUGS analogues. At first glance, in terms of both radial dependence and amplitude, the HI surface density profiles of the MaGICC discs resemble very closely those shown in Fig 23 of O’Brien et al. (2010). It is important to bear in mind though that the O’Brien et al. profiles were inferred (necessarily) from observations of edge-on discs. Our analysis of the simulations is restricted to face-on orientations, and so a fairer comparison would be to the sample of Bigiel & Blitz (2012), who derived both HI and  $H_2$  surface density profiles for a sample of face-on galaxies observed by THINGS.

Bigiel & Blitz (2012) show that the HI in such disc galaxies is distributed more uniformly, in terms of surface density, out to  $\sim 10$  kpc, with (roughly) only a factor of  $\sim 3$  decline in going to a galactocentric radius of  $\sim 20$  kpc. This is consistent with the flatter gradient seen for the MUGS simulations, albeit the issue of their aforementioned overly truncated ‘edges’ remains. Because we cannot resolve the transition from HI to  $H_2$  in our simulations, some fraction of what is labelled as ‘HI’ in Fig 2 (at least within the inner 5–10 kpc, for the MaGICC simulations, where the surface density is close to, or exceeds, the empirical upper limit for HI in nature) could certainly be misidentified  $H_2$ , and so our inner gradients would be somewhat flatter than presented and therefore more consistent with the profiles of Bigiel & Blitz for radii  $\lesssim 10$  kpc. Our predicted HI surface density gradients in the  $\sim 10\text{--}20$  kpc range are (on average) somewhat steeper than the typical galaxy from Bigiel & Blitz (in the same radial range - see their Fig 1a), but certainly lie within  $\sim 1\sigma$  of the distribution. In that sense, the extended nature and (outer disc) exponential profiles of the MaGICC simulations are more consistent with those encountered in nature.

<sup>4</sup> [www-hpcc.astro.washington.edu/tools/tipsy/tipsy.html](http://www-hpcc.astro.washington.edu/tools/tipsy/tipsy.html)

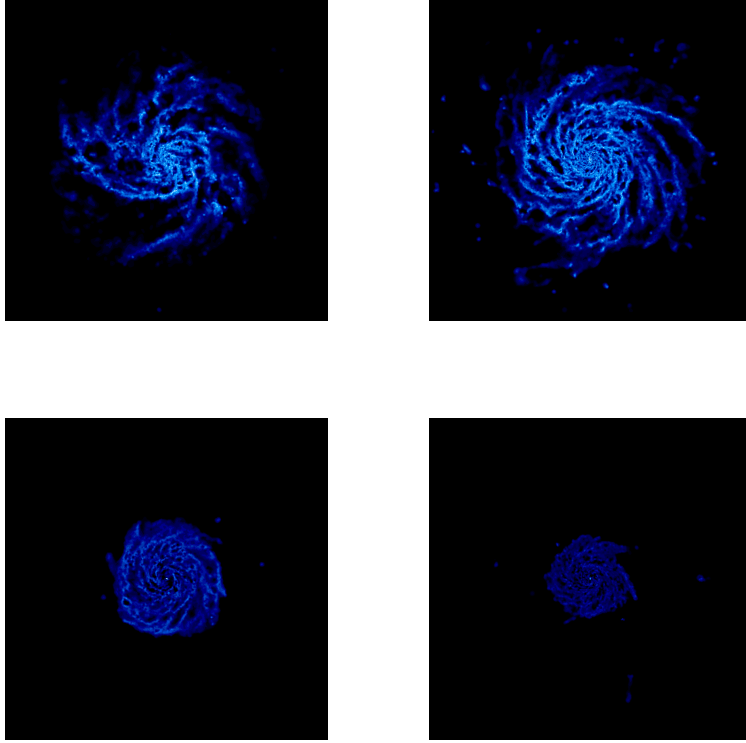


**Figure 1.** Zeroth-moment HI maps for our four simulated  $\sim L^*$  late-type discs: g1536-MaGICC (upper-left); g15784-MaGICC (upper-right); g1536-MUGS (bottom-left); g15784-MUGS (bottom-right). Each panel spans  $100 \times 100$  kpc, with a column density range of  $10^{19} \text{ cm}^{-2}$  to  $10^{21} \text{ cm}^{-2}$  (comparable to the limits imposed by 21cm surveys such as THINGS).

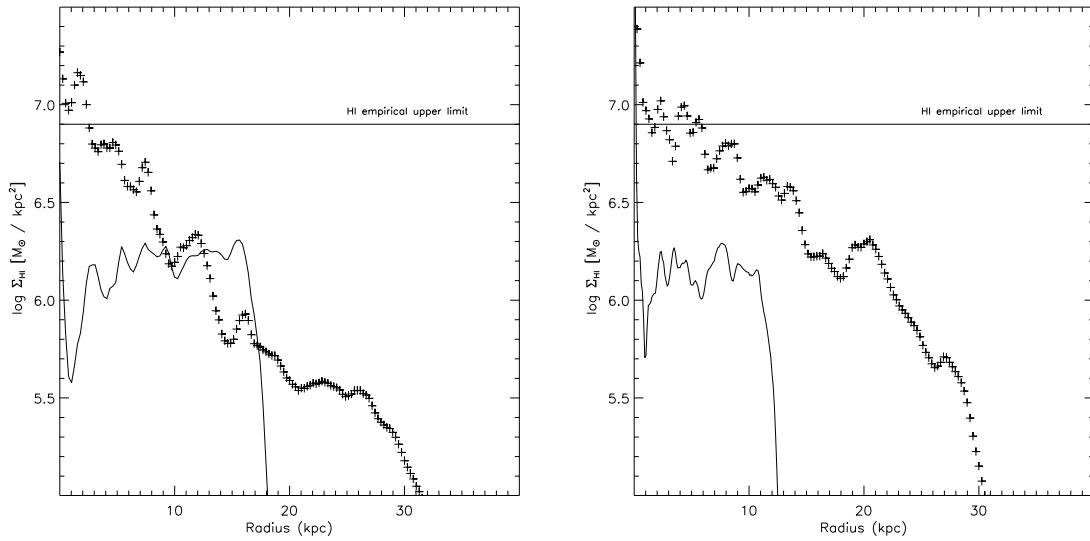


**Figure 2.** Radial HI surface density profiles for the g1536 (left panel) and g15784 (right panel) simulations. The plus symbols represent the MaGICC runs and the solid lines correspond to the MUGS runs. The solid horizontal line in each panel correspond to the empirical HI upper limit from Bigiel et al. (2008).

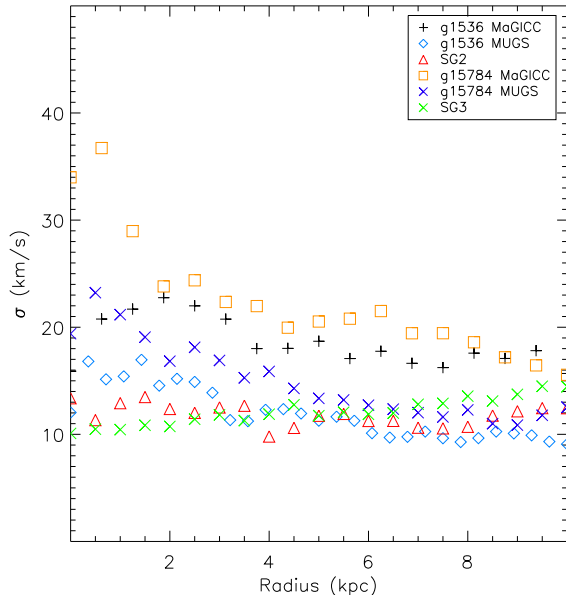


**Figure 3.** Line-of-sight velocity dispersion profiles for the HI within the face-on representations of g1536-MaGICC (black plus symbols); g1536-MUGS (blue diamonds); g15784-MaGICC (red triangles); g15784-MUGS (orange squares); SG2 (blue crosses), and SG3 (green crosses).

### 3.3 Radial Velocity Dispersion Profiles

The radial HI velocity dispersion profiles derived from the second-moment maps (Fig 3) present fairly ‘flat’ trends with increasing galactocentric distance, save for perhaps g15784, with  $\sigma$  decreasing typically by  $\sim 50\%$  in going from the inner disc to a galactocentric radius of  $\sim 10$  kpc; the profiles for the dwarfs (SG2 and SG3) are flat over this radial range, consistent with the dwarfs shown in Fig 3 of Pilkington et al (2011). Here, as the second-moment maps are for face-on viewing angles, the velocity dispersions quoted in Fig 3 are equivalent to  $\sigma_w$ . We are only showing the velocity dispersion profiles within the star-forming parts of the disks (i.e., radii  $\lesssim r_{25}$  for the massive MaGICC and MUGS discs, and  $\lesssim 2r_{25}$  for the lower mass dwarfs SG2 and SG3, where  $r_{25}$  is the isophotal radius corresponding to 25 mag arcsec $^{-2}$ ). As such, the dispersions being  $\sim 20\text{--}100\%$  higher than the ‘characteristic’ value outside the star-forming disc ( $\sim 10$  km/s; Tamburro et al 2009) is not entirely unexpected.

The three main conclusions to take from this part of the analysis are that: (i) the profiles and amplitudes for the velocity dispersions of the cold gas *within the star-forming region* of the four massive MUGS and MaGICC discs overlap with those encountered in nature (Fig 1 of Tamburro et al.); (ii) the flat profiles of the two dwarfs (SG2 and SG3) are more problematic, consistent with the conclusions of Pilkington et al. (2011), and reflecting a limitation of our inability to resolve molecular hydrogen processes on these scales; (iii) the amplitudes of the MaGICC variants, relative to their MUGS counterparts, are  $\sim 50\%$  higher (although both are within the range encountered in nature); such a result is not

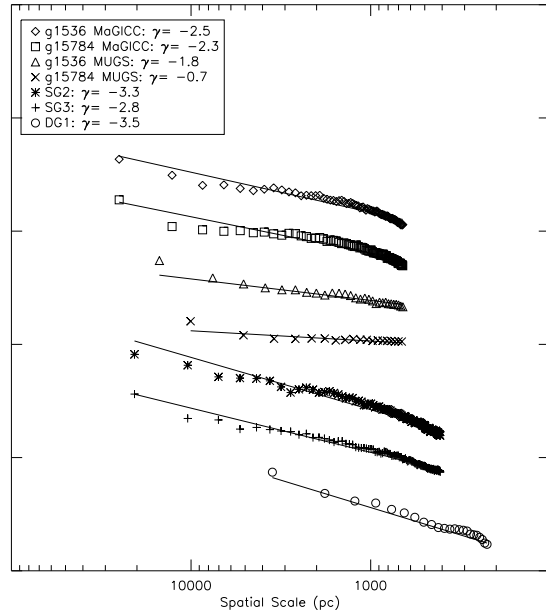


**Figure 4.** Power spectra for the four  $\sim L^*$  MaGICC and MUGS simulations (upper four spectra), two ‘dwarf’ variants of g1536 and g15784 (SG2 and SG3, respectively), and the low-mass dwarf DG1, from Pilkington et al. (2011). The inset within the panel links the symbol with the relevant simulation. The ordinate represents arbitrary units of spatial power, as the relative distribution (rather than absolute) is the focus of this work; each spectrum has been offset with respect to the next, for ease of viewing.

entirely unexpected, given the significantly enhanced feedback associated with the MaGICC runs.

### 3.4 Power Spectra

As noted in §2.2, power spectra were derived from each of the simulated and empirical (THINGS) HI moment-zero maps, by averaging in circular annuli in frequency space after Fourier transforming the images. The technique is identical to that employed by Stanimirovic et al. (1999) and Pilkington et al. (2011). While alternate approaches certainly exist (cf. Dutta et al. 2013), we are more concerned here with adopting a homogeneous approach for both the simulations and the data, rather than necessarily inter-comparing the various techniques available.

Fig 4 shows the power spectra for both the MaGICC and MUGS variants of g1536 and g15784 simulations, as well as their respective dwarf galaxy analogs, SG2 and SG3. For each of the four massive discs’ spectra, single power-law fits are shown (solid curves) for the spatial scales over which the fits were derived ( $\sim 0.6\text{--}2$  kpc). It should be emphasised that the lower limit on the spatial scale over which these fits were made corresponds to twice the softening length employed in the simulations; while an argument could be made to extending to somewhat smaller scales, we felt it prudent to be conservative in our analyses. What can hopefully be appreciated from a cursory analysis of Fig 4 is the relatively enhanced power on sub-kpc scales seen in MUGS (conventional feedback) realisations, compared with their MaGICC (enhanced feedback) analogues. This is reflected in the

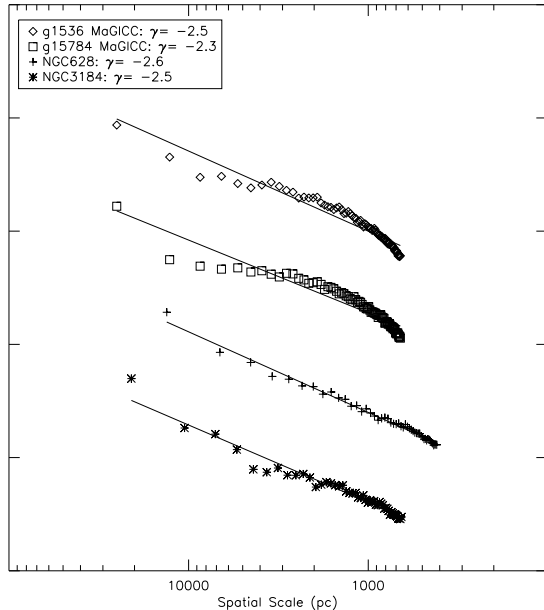


**Figure 5.** Power spectra for the two MaGICC simulations, and two selected from the empirical THINGS dataset (NGC 628 and 3184). All other details are as per the caption to Fig 4.

single power-law slopes itemised in the inset to the panel (which are weighted heavily by the more ‘numerous’ higher frequency ‘bins’ on sub-kpc scales), which are meant to be illustrative here, rather than represent the formal ‘best fit’ to the data. Broadly speaking, the power spectra are roughly an order of magnitude steeper when using the MaGICC feedback scheme, as opposed to that of MUGS - i.e., *it appears that the stronger feedback shifts the ISM power from predominantly ‘small’ ( $\lesssim 1$  kpc) to large ( $\gtrsim 2$  kpc) spatial scales.*

We next extended our analysis to lower mass, late-type, systems, including the two dwarf variants to g1536-MaGICC and g15784-MaGICC (referred to as SG2 and SG3, as per Brook et al. 2012). We also performed an independent re-analysis of the dwarf (DG1) that formed the basis of our earlier work (Pilkington et al. 2011). The inclusion of these three ‘dwarfs’ allows us to push the analysis to somewhat smaller spatial scales, while still working within a framework of ‘enhanced’ feedback. The power spectra for all seven systems are shown in Fig 4. An important conclusion to be drawn from this figure (and associated quoted single power-law fits within the inset to the panel) is that *on  $\sim$ sub-kpc scales, the power spectra slopes of the three dwarfs (SG2, SG3, DG1) are steeper ( $-3.5 \lesssim \gamma \lesssim -3$ ) than their more massive analogues.*

We then compared the predicted power spectra from the two  $\sim L^*$  discs realised with the enhanced MaGICC feedback scheme, with those derived from galaxies from the THINGS database; the full database is shown in Fig 7, but for succinctness, we only show the power spectra for NGC 628 and 3184 (which were chosen, in part, because they were the closest to face-on, matching, by construct, the MaGICC simulations), alongside the MaGICC discs, in Fig 5. In terms of formal single power-law fits to these spectra, the MaGICC and (selected) THINGS galaxies are very similar (as shown by the quoted slopes within the inset to the panel). Having

said that, as already alluded to in relation to Fig 4, the MaGICC spectra do not appear entirely consistent with a single power-law, instead presenting evidence for something of a ‘break’ in the structural power, on the scales of  $\sim 1$ – $2$  kpc (being flatter on larger scales, and steeper on smaller scales, a point to which we return below).

Inspection of Figs 4 and 5 suggests that single power law fits are not necessarily the best option. In Fig 6, we show the result of performing two-component fits to both the MaGICC data and a selected galaxy from THINGS (NGC 2403, chosen as it is the THINGS galaxy whose power spectrum looks like it would suit a 2-component fit best). In a qualitative sense, the behaviour is not dissimilar - i.e., both the MaGICC simulations and NGC 2403 show flatter power spectra on larger scales, compared with smaller scales, although the transition from ‘flat’ to ‘steep’ occurs at  $\sim 2$  kpc in the simulations, as opposed to  $\sim 0.5$  kpc in NGC 2403. This seems to be consistent with the idea posed by Dutta et al. (2013) that there is a steep power-law component on smaller scales driven by 3-dimensional turbulent motions, which flattens at larger spatial scales. At these larger scales, 2-dimensional turbulent motions begin to dominate within the plane of the galactic disc. The steepening of the power spectra on small spatial scales observed in the power spectra of the MaGICC large discs is also seen in work undertaken by Elmegreen et al. (2001) in their work on the LMC.

Power spectra have been generated for the 17 THINGS galaxies employed in the analysis of Dutta et al. (2013); these are provided in the accompanying Appendix as Fig 7. The majority have slopes on the order of  $\gamma \sim -2.3$  to  $-2.8$ , with two exceptions: NGC 3031 ( $\gamma \sim -0.9$ ) and NGC 3521 ( $\gamma \sim -3.3$ ). Much as for the simulations, the point associated with the largest spatial scales in each panel should be viewed with some skepticism, as edge effects do come into play (i.e., the ‘edge’ of the HI disc is ‘seen’ as a high power ‘scale’ against an almost noise-free background).

## 4 CONCLUSIONS

We have presented an analysis of the cold gas and HI content of simulated discs with both ‘standard’ (MUGS) and ‘enhanced’ (MaGICC) energy feedback schemes, as well as re-scaled dwarf variants of the massive (MaGICC) simulations.

Radial density profiles were generated for the MUGS and MaGICC  $\sim L^*$  variants of g1536 and g15784 (Fig 2). These were generated using their respective zeroth HI moment maps; the weaker feedback associated with MUGS resulted in very flat radial HI distributions, with sharp cut-offs at galactocentric radii of  $\sim 12$ – $15$  kpc, while the stronger feedback associated with MaGICC resulted in HI discs with exponential surface density profiles (with scalelengths of  $\sim 6$ – $8$  kpc) which were  $\sim 2$ – $3\times$  more extended (at an HI column density limit of  $\sim 10^{19} \text{ cm}^{-2}$ ). The exponential profiles exhibited by the enhanced feedback runs are consistent with the typical profile observed in nature (Bigiel et al. 2008; O’Brien et al. 2010). The majority of the THINGS radial density profiles show evidence of exponential components, indicating that the MaGICC simulations distribute

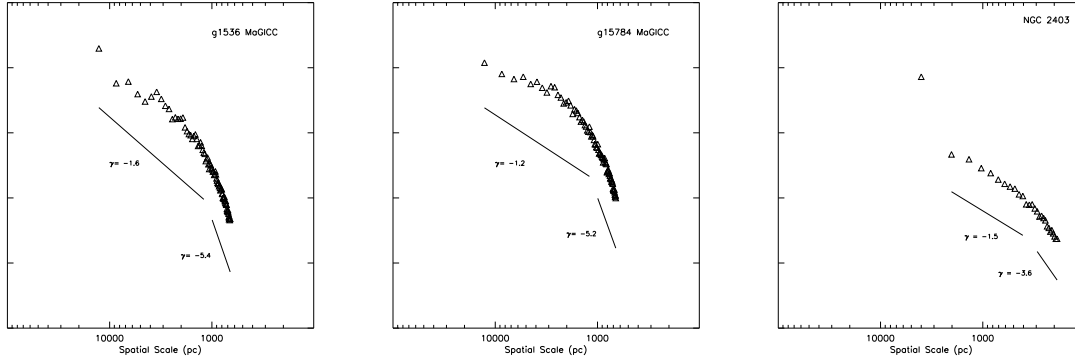


**Figure 6.** Power spectra of g1536-MaGICC, g15784-MaGICC, and NGC 2403, respectively (from left to right). Each spectrum appears (in a qualitative sense) inconsistent with a single power-law fit; two-component fits, with a shallower (steeper) slope on larger (smaller) scales, are suggested, although the ‘knee’ in the spectra occurs on different scales for the simulations ( $\sim 2$  kpc), as opposed to that of NGC 2403 ( $\sim 0.5$  kpc).

the column density in a way that better matches observational evidence.

The power spectra generated for the massive ( $\sim L_\star$ ) discs with enhanced (MaGICC) feedback are steeper than their weaker (MUGS) feedback counterparts. In other words, the stronger feedback shifts the power in ISM from smaller scales to larger scales. Forcing a single component power-law to the MaGICC spectra yields slopes consistent with similarly forced single component fits to the empirical THINGS spectra, also well-described by a single component power law; having said that, the MaGICC spectra are more consistent with a two-component structure, with a steeper slope on sub-kpc spatial scales, flattening to shallower slopes on larger scales. The massive discs realised with the MUGS feedback scheme are both shallower than MaGICC, but also well-fit with a single power-law across all spatial scales. The dwarf galaxies realised in our work with enhanced feedback possess steeper slopes than their more massive counterparts, with values that are in agreement with Stanimirovic et al. (1999) and Pilkington et al. (2011).

It is arguable that several of the THINGS power spectra warrant multiple-component fits (namely NGC 2403, 3031, 3184, 3198 and 7793) and the multi-component fits performed on NGC 2403 and the two large disc MaGICC galaxy power spectra indicate that the large-scale slopes agree well, whereas the small scale slopes differ largely. This indicates that the MaGICC feedback scheme distributes HI structures on a scale that is comparable to those of observational results, but there is a lack of small-scale structure. It is apparent that there is no 1:1 match to the THINGS data from either the MUGS or MaGICC feedback schemes, but MaGICC appears to fare better than the MUGS feedback scheme from a single-component fit in an average sense. The lack of a 1:1 relation may be largely due to the challenges in converting from ‘cold gas’ to ‘HI’ as well as a lack of exactly face-on systems observed in nature and in the THINGS survey.

## ACKNOWLEDGMENTS

BKG acknowledges the support of the UKs Science & Technology Facilities Council (ST/J001341/1). KP acknowledges

the support of STFC through its PhD Studentship programme (ST/F007701/1). The generous allocation of resources from STFCs DiRAC Facility (COSMOS: Galactic Archaeology), the DEISA consortium, co-funded through EU FP6 project RI-031513 and the FP7 project RI-222919 (through the DEISA Extreme Computing Initiative), the PRACE-2IP Project (FP7 RI-283493), and the University of Central Lancshires High Performance Computing Facility.

## REFERENCES

- Bigiel F., Blitz L., 2012, *ApJ*, 756, 183
- Bigiel F., Leroy A., Walter F., Brinks E., de Blok W. J. G., Madore B., Thornley M. D., 2008, *AJ*, 136, 2846
- Brook C. B., Kawata D., Gibson B. K., Flynn C., 2004, *MNRAS*, 349, 52
- Brook C. B., Stinson G., Gibson B. K., Wadsley J., Quinn T., 2012, *MNRAS*, 424, 1275
- Calura F., Gibson B. K., Michel-Dansac L., Stinson G. S., Cignoni M., Dotter A., Pilkington K., House E. L., Brook C. B., Few C. G., Bailin J., Couchman H. M. P., Wadsley J., 2012, *MNRAS*, 427, 1401
- Chabrier G., 2003, *PASP*, 115, 763
- Combes F., Boquien M., et al. 2012, *A&A*, 539, A67
- Durier F., Dalla Vecchia C., 2012, *MNRAS*, 419, 465
- Dutta P., Begum A., Bharadwaj S., Chengalur J. N., 2013, *New A*, 19, 89
- Elmegreen B. G., Kim S., Staveley-Smith L., 2001, *ApJ*, 548, 749
- Gibson B. K., Pilkington K., Brook C. B., Stinson G. S., Bailin J., 2013, *A&A*, 554, A47
- Governato F., Brook C., Mayer L., Brooks A., Rhee G., Wadsley J., Jonsson P., Willman B., Stinson G., Quinn T., Madau P., 2010, *Nature*, 463, 203
- Hambleton K. M., Gibson B. K., Brook C. B., Stinson G. S., Conselice C. J., Bailin J., Couchman H., Wadsley J., 2011, *MNRAS*, 418, 801
- Hopkins P. F., Cox T. J., Hernquist L., Narayanan D., Hayward C. C., Murray N., 2013, *MNRAS*, 430, 1901
- House E. L., Brook C. B., Gibson B. K., Sánchez-Blázquez P., Courty S., Few C. G., Governato F., Kawata D.,

- Roškar R., Steinmetz M., Stinson G. S., Teyssier R., 2011, MNRAS, 415, 2652
- Kroupa P., Tout C. A., Gilmore G., 1993, MNRAS, 262, 545
- Macciò A. V., Stinson G., Brook C. B., Wadsley J., Couchman H. M. P., Shen S., Gibson B. K., Quinn T., 2012, ApJ, 744, L9
- O'Brien J. C., Freeman K. C., van der Kruit P. C., 2010, A&A, 515, A62+
- Pilkington K., Few C. G., Gibson B. K., Calura F., Michel-Dansac L., Thacker R. J., Mollá M., Matteucci F., Rahimi A., Kawata D., Kobayashi C., Brook C. B., Stinson G. S., Couchman H. M. P., Bailin J., Wadsley J., 2012, A&A, 540, A56
- Pilkington K., Gibson B. K., Brook C. B., Calura F., Stinson G. S., Thacker R. J., Michel-Dansac L., Bailin J., Couchman H. M. P., Wadsley J., Quinn T. R., Maccio A., 2012, MNRAS, 425, 969
- Pilkington K., Gibson B. K., Calura F., Brooks A. M., Mayer L., Brook C. B., Stinson G. S., Thacker R. J., Few C. G., Cunnamana D., Wadsley J., 2011, MNRAS, 417, 2891
- Scannapieco C., Wadepuhl M., et al. 2012, MNRAS, 423, 1726
- Schaye J., Dalla Vecchia C., Booth C. M., Wiersma R. P. C., Theuns T., Haas M. R., Bertone S., Duffy A. R., McCarthy I. G., van de Voort F., 2010, MNRAS, 402, 1536
- Shen S., Wadsley J., Stinson G., 2010, MNRAS, 407, 1581
- Stanimirovic S., Staveley-Smith L., Dickey J. M., Sault R. J., Snowden S. L., 1999, MNRAS, 302, 417
- Stinson G. S., Bailin J., Couchman H., Wadsley J., Shen S., Nickerson S., Brook C., Quinn T., 2010, MNRAS, 408, 812
- Stinson G. S., Brook C., Macciò A. V., Wadsley J., Quinn T. R., Couchman H. M. P., 2013, MNRAS, 428, 129
- Stinson G. S., Brook C., Prochaska J. X., Hennawi J., Shen S., Wadsley J., Pontzen A., Couchman H. M. P., Quinn T., Macciò A. V., Gibson B. K., 2012, MNRAS, 425, 1270
- Thacker R. J., Couchman H. M. P., 2000, ApJ, 545, 728
- Wadsley J. W., Stadel J., Quinn T., 2004, New Astronomy, 9, 137
- Walter F., Brinks E., de Blok W. J. G., Bigiel F., Kennicutt R. C., Thornley M. D., Leroy A., 2008, AJ, 136, 2563

## APPENDIX

We present here the ISM power spectra for the 17 THINGS galaxies used in this work. The inset to each panel includes the galaxy name, the weighting scheme employed (RO=robust), and the best-fit (single component) power-law slope.



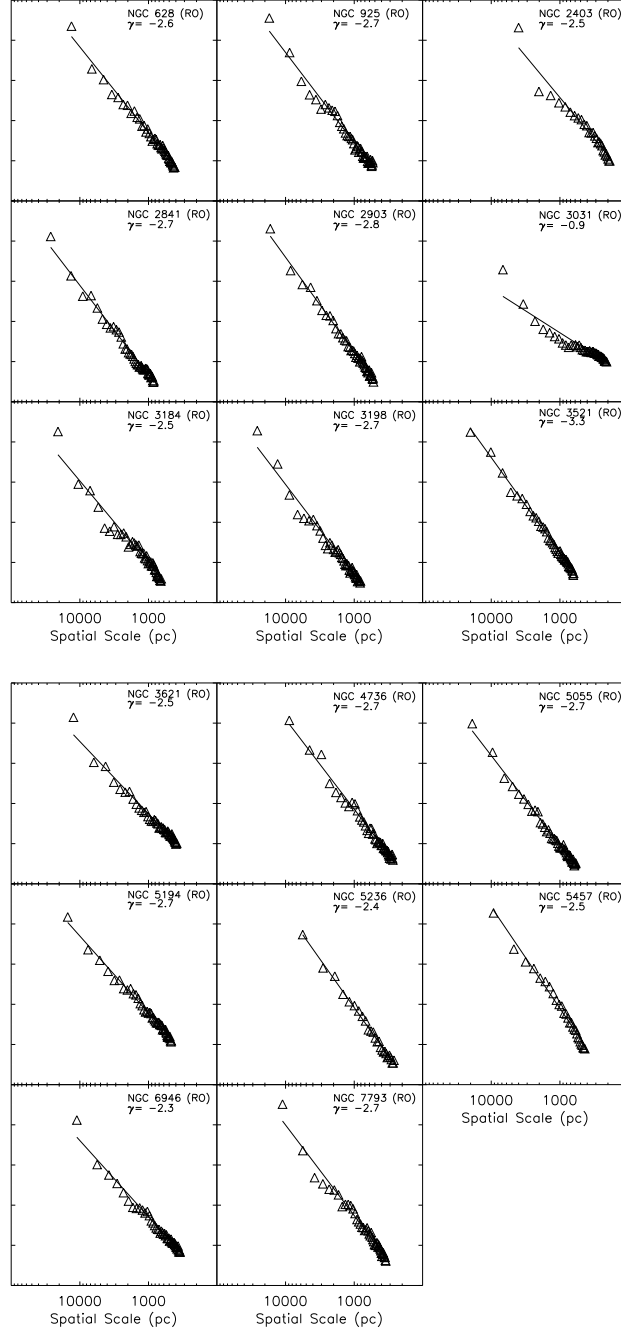


**Figure 7.** Power spectra for all the THINGS galaxies analysed in this work; names of the galaxies are listed on their corresponding plots along with the power law slope value. The power law slope is plotted over the points as a solid line.